

A 3D NUMERICAL SIMULATION OF CORNER
BREAKDOWN IN EXTENDED-DRAIN MOSTS
D. J. COE,
Philips Research Laboratories,
Redhill, Surrey, RH1 5HA, England
H. N. G. VAES,
Philips Development Laboratories,
Nijmegen, The Netherlands.

ABSTRACT

The presence of external and internal angles on the mask layout for lightly-doped extended-drain MOSTs can cause marked 3D corner effects. In the present work, the 2/3D simulation package, TRIPPOS, is used to study the effect of interdigititation on the design of a MOS tetrode transistor.

1. INTRODUCTION

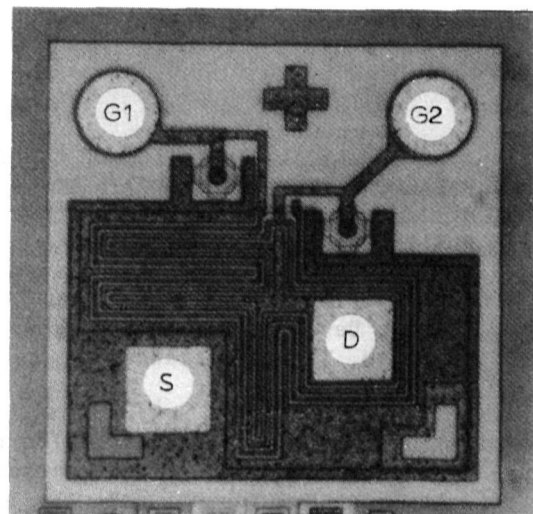
The maximum operating voltage of conventional MOS transistors with highly-doped drains is determined, in most cases, by avalanche breakdown (1) or charge injection (2) in the high-field drain-corner region. However, this voltage can be increased considerably if a lightly-doped drain-extension is used in the critical region of gate-drain overlap (3,4). In addition, preferential depletion of this drain-extension acts to suppress short-channel effects.

The design of such devices has, in the past, made use of 2D numerical simulation (3). For many surface geometries this approach is adequate; there are, however, a number of instances (for example, interdigitated cell structures) where marked 3D corner effects must be taken into account.

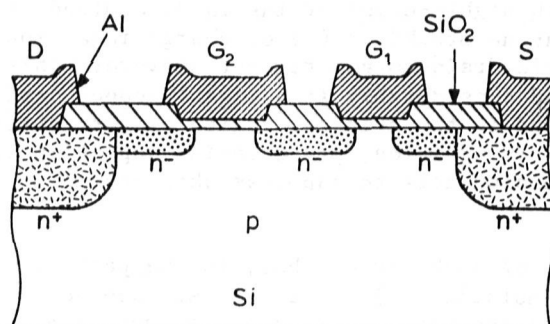
In this paper the 3D semiconductor simulation package, TRIPPOS(5), is used to study such effects in an interdigitated MOS tetrode transistor. The results, however, are relevant to other MOSTs with lightly-doped extended-drains.

2. DEVICE STRUCTURE

The device topography for the interdigitated MOST tetrode is shown in Figure 1(a) and its corresponding schematic cross-section in Figure 1(b).



(a)



(b)

Fig.1. (a) Device topography and (b) schematic cross-section for MOST tetrode

A 3D NUMERICAL SIMULATION OF CORNER BREAKDOWN
IN EXTENDED-DRAIN MOSTS

123

The fabrication is based on an aluminium-gate process with the lightly-doped n⁻ regions auto-aligned with the thick field oxide, either by out diffusion from appropriately-defined phosphorus-doped glass or by overall arsenic implantation with subsequent local silicon removal and regrowth of the gate oxide. Typical device dimensions and material parameters are shown in Table 1.

For normal device operation, the critical area for avalanche breakdown will occur in the overlap region between G₂ and the n drain extension. The surface view shows the interdigititation to give both internal and external corners to this (already sensitive) region of the device.

Table 1
Typical Device Parameters

Substrate doping	10 ¹⁵ cm ⁻³
Field oxide thickness	0.8 μm
Gate oxide thickness	0.052 μm
n ⁻ junction depth	0.3 μm
n ⁺ junction depth	2.0 μm
1st gate width	1.8 μm
2nd gate width	3.2 μm

3. NUMERICAL SIMULATION

For purposes of simulation the lower voltage portions of the MOST tetrode (the source and G₁ regions) were ignored and the study of 3D corner effects carried out only for the higher voltage MOST section (G₂ and the extended-drain). Since the lengths of the interdigitated tracks were reasonably long compared with their widths, the external and internal n⁻ corners were analysed separately using the plan views and cross-section of Figures 2(a) - (c).

Off-state simulation was carried out with the substrate, the internal n node and the second gate at zero potential. The diffusion profiles were assumed to be gaussian perpendicular to the device surface (with the peak concentration located at the oxide-semiconductor interface) and to follow a complementary error function parallel to the device surface (with the half-amplitude point aligned with the diffusion mask).

Equipotential contours for conventional 2D simulation of the MOST cross-section of Figure 2(c) are shown in Figures 3(a) and (b). The operation of the extended-drain is typified by the increase in the degree of depletion in the gate-drain overlap region of the n⁻ extension as the surface

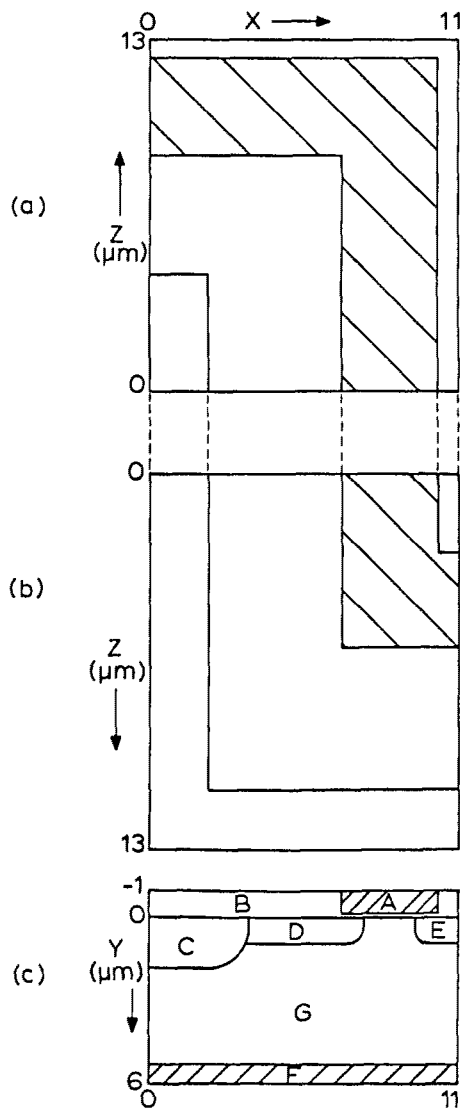


Fig. 2. Mask geometry of a) external corner,
b) internal corner with c) end view of device.

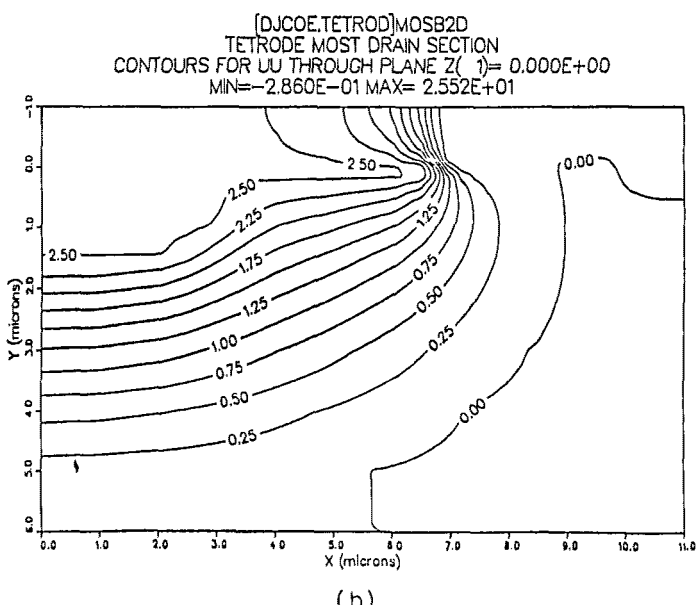
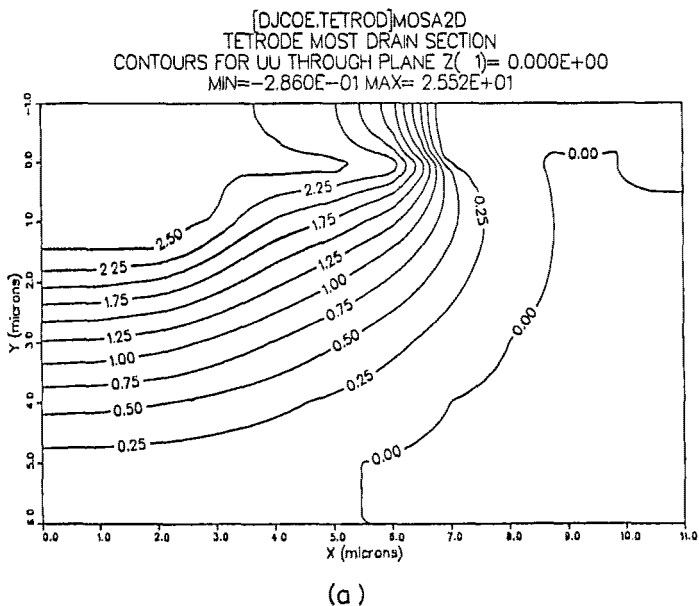


Fig.3. Equipotential contours for n^- surface concentrations of a) $2.10^{17} \text{ cm}^{-3}$ and b) $5.10^{17} \text{ cm}^{-3}$ (2D simulation).

concentration is decreased from $5.10^{17} \text{ cm}^{-3}$ (Figure 3(b)) to $2.10^{17} \text{ cm}^{-3}$ (Figure 3(a)). The consequent lowering of the peak field in the crucial overlap region is illustrated in Figures 4(a) and (b).

Equivalent 3D simulation of both external and internal n⁻ corner sections of the device (Figures 2(a) and (b) respectively) yield results that are, at first sight, unexpected. These results are shown in Figures 5 to 7 and give plots of total field in planes parallel to the device surface. The view for the external n⁻ (Figures 5(a) to 7(a)) is taken from the n⁺ drain looking towards the gate; that for the internal n⁻ corner (Figures 5(b) to 7(b)) is taken from the n⁻ internal node looking towards the gate.

In a plane just below the oxide-semiconductor interface (Figures 5 and 7), the total field at the apex of the n⁻ corner dips for the external angle and peaks for the internal angle. The extent of this 3D field anomaly depends on the doping level of the n⁻ drain extension, being approximately 2.5 μm for an n⁻ surface concentration of $5.10^{17} \text{ cm}^{-3}$ (Figure 5) and only some 0.25 μm for a value of $2.10^{18} \text{ cm}^{-3}$ (Figure 7).

It is clear from these results that the field at the apex of the n⁻ corner is dominated by the acuteness of the angle of the gate track rather than by that of the diffusion. The converse is true at the apex of the n⁺ corner in a similar plane parallel to the surface but deeper into the device (Figure 6(a) and (b)). In this case, the field peaks at the acute, external n⁺ corner and dips at the obtuse, internal n⁺ corner.

The behaviour of the various sections of the n⁻ drain extension is clarified further by the change in the hole ionisation integral with n⁻ surface concentration, as shown in Figure 8. These are calculated using the ionisation coefficients of Overstraeten and de Man (6). For low n⁻ doping concentrations, the field peak for the internal n⁻ corner (3D) leads to a considerable increase in ionisation integral compared with the (essentially identical) values along the edge of the device (2D) and at the external n⁻ corner (3D). As the doping is further increased, the field peak at the apex of the internal n⁻ corner remains; however, the length of the path of steepest descent through this field peak decreases markedly. The net ionisation integral through the peak (marked by the dotted curve in Figure 8) decreases, therefore, with respect to those through the local maxima along the edge of the device (marked by the solid curve). The short avalanche path between the undepleted drain-diffusion and the oxide-semiconductor interface is typical of drain-corner breakdown for conventional MOSTs. Its

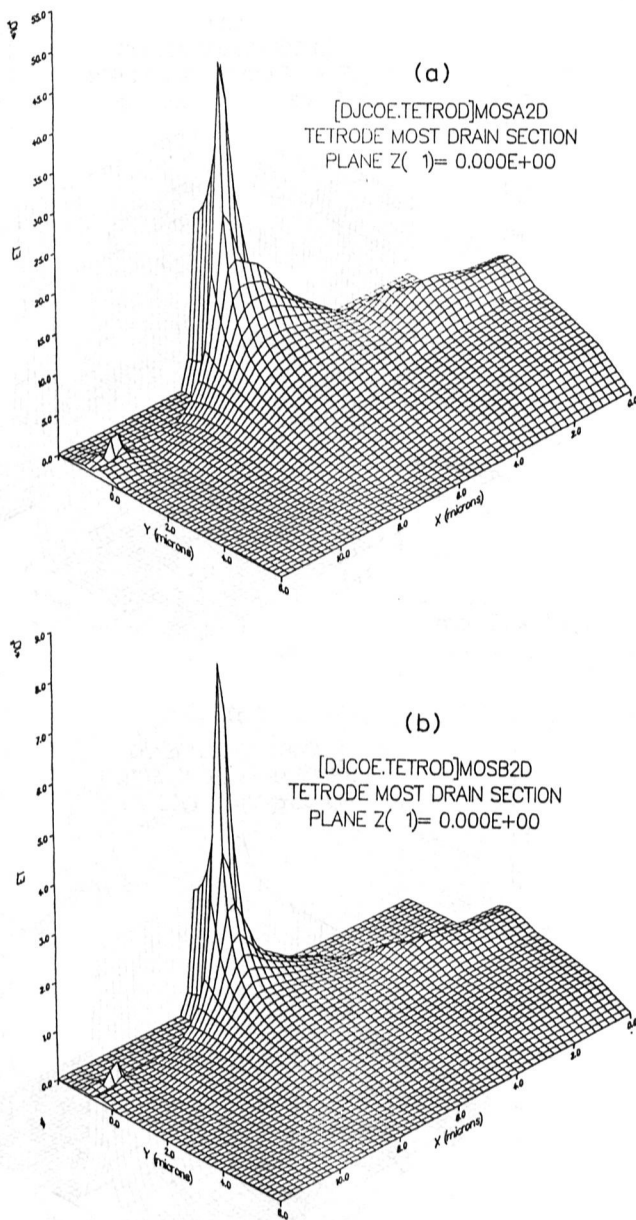


Fig.4. Field distribution for n^- surface concentrations of a) 2.10^{17}cm^{-3} and b) 5.10^{17}cm^{-3} (2D simulation).

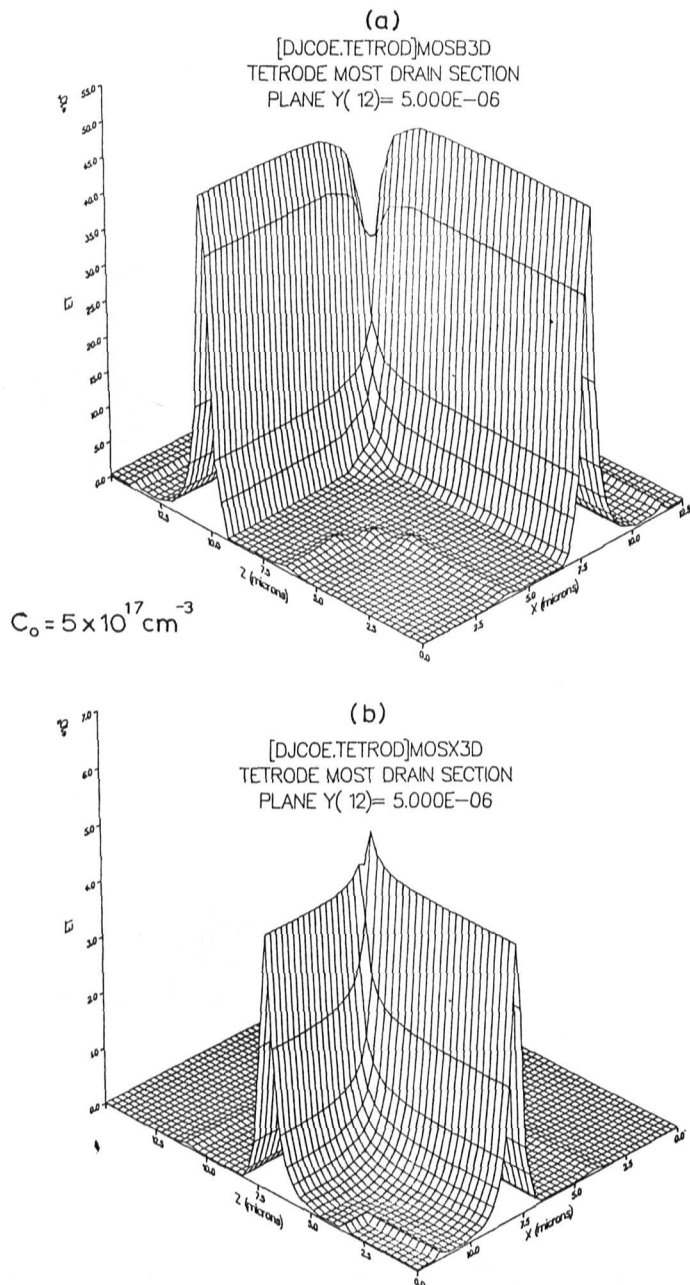


Fig.5. Field distribution through the n^- junction in a plane parallel to the surface for 3D simulation of
a) the external and b) the internal n^- corners

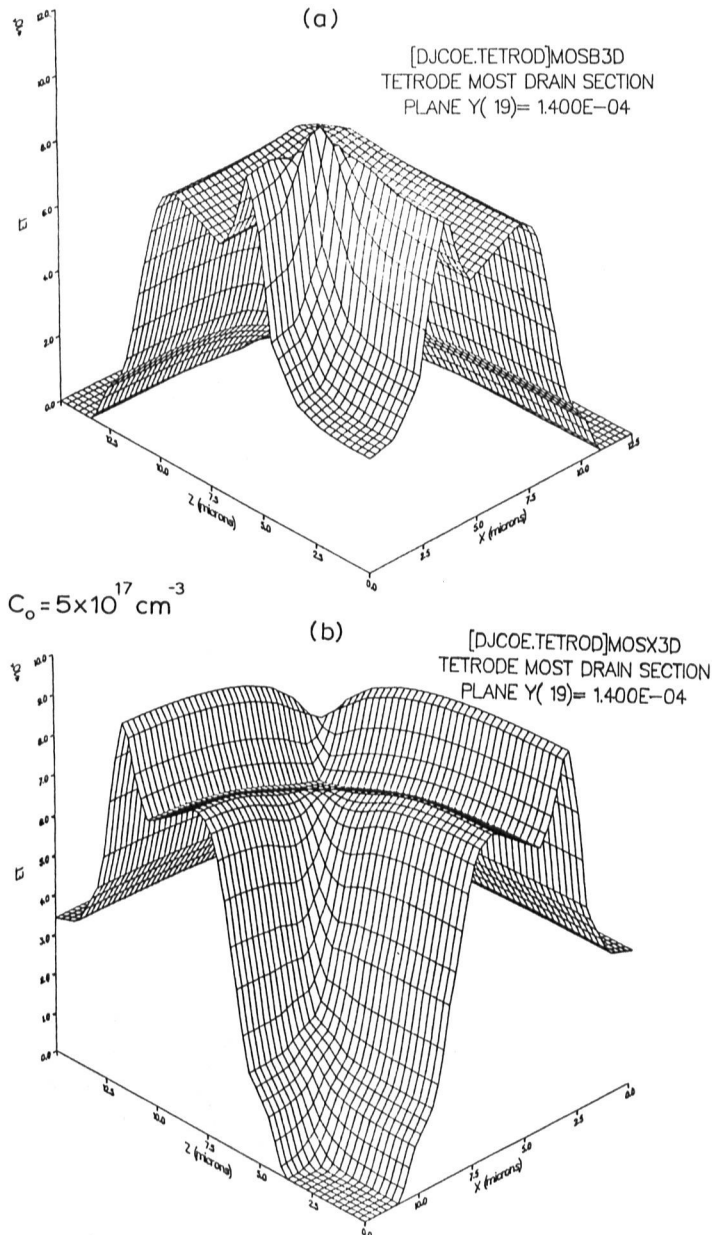


Fig.6. Field distribution through the n^+ junction in a plane parallel to the surface for 3D simulation of a) the external and b) the internal n^- corners.

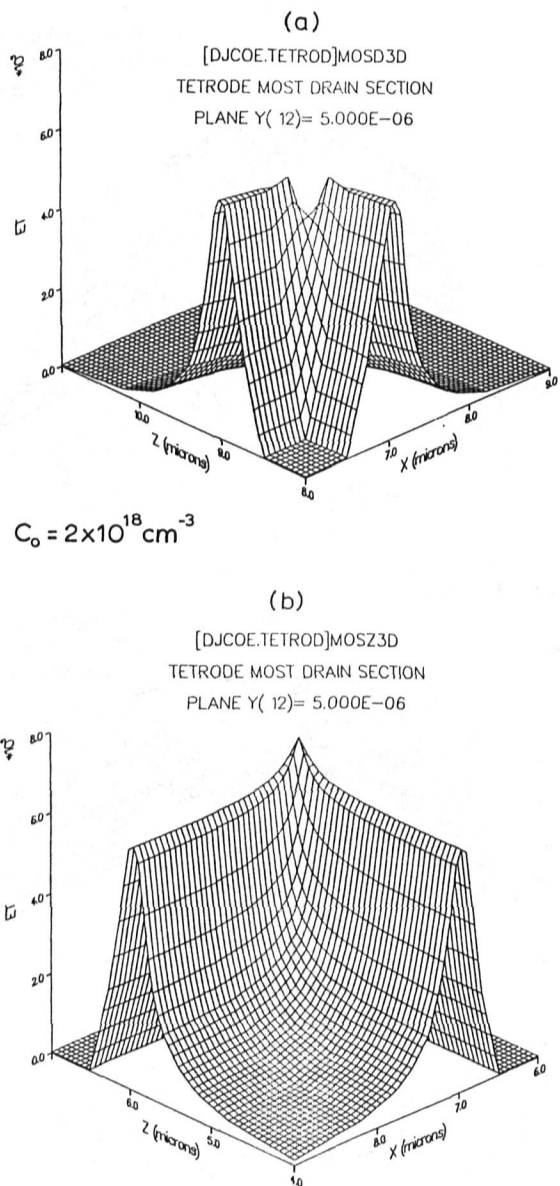


Fig. 7. Field distribution through the n^- junction in a plane parallel to the surface for 3D simulation of
a) the external and b) the internal n^- corners.

A 3D NUMERICAL SIMULATION OF CORNER BREAKDOWN
IN EXTENDED-DRAIN MOSTS

131

associated ionisation integral is somewhat susceptible to small numerical inaccuracies during device simulation, and the spread in values for ionisation integral for the highest doping level is linked with this.

Finally, the effect of the various 3D corners on device breakdown is given in Figure 9. Both 2D and 3D external n⁻ corner simulations give similar results, being dominated by breakdown along the device edges. The presence of internal n⁻ corners, however, has a marked deleterious effect on breakdown voltage. The maximum attainable voltage with sufficient decrease in n⁻ doping is limited by the length of the drain extension. For given values below this maximum, however, the doping (and hence the series conductance) of the drain extension can be considerably reduced by the need to compensate for internal n⁻ corner breakdown.

4. CONCLUSIONS

3D numerical simulation of an interdigitated MOST tetrode has revealed a (perhaps unsuspected) problem in the design of this and other related extended-drain structures.

For conventional MOSTs with highly-doped drains, drain-corner avalanche breakdown is dominated by the thickness of the gate oxide. Other factors, such as 3D corner effects caused by cell geometry or interdigititation are of secondary importance.

However, where the desired breakdown voltage has been increased through use of lightly-doped drain extensions, preferential breakdown can occur at the corners of the interdigitation where an acute gate track angle overlies an internal corner of the drain diffusion. Since reduction of this field peak via further decrease in drain doping can substantially increase the parasitic drain resistance, steps must be taken to avoid or to radius such internal diffusion corners.

6. REFERENCES

- (1) DE GRAAFF, H. C., Philips Res. Rep., 25, 21 (1970)
- (2) NING, T. H., OSBURN, C. M. & YU, H. N., Appl. Phys. Lett., 29, 198 (1976)
- (3) COE, D. J. & BROCKMAN, H. E., Solid-St. Electron., 22, 443 (1979)
- (4) OGURA, S., TSANG, P. J., WALKER, W., CRITCHLOW, D. & SHEPART, J. F., IEEE Trans., ED27, 1359 (1980)
- (5) COE, D. J., WHIGHT, K. R., TREE, R. J. & VEVERIS, A. J., Proc. NASECODE III, p. 102, Galway, 1983

- (6) VAN OVERSTRAETEN, R & DE MAN, H., Solid-St.
Electron., 13, 583 (1970)

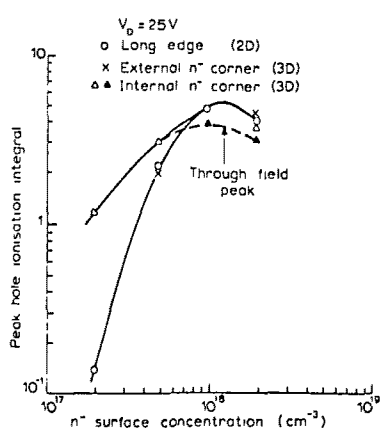


Fig 8 Peak hole ionisation integral v. n^- surface concentration

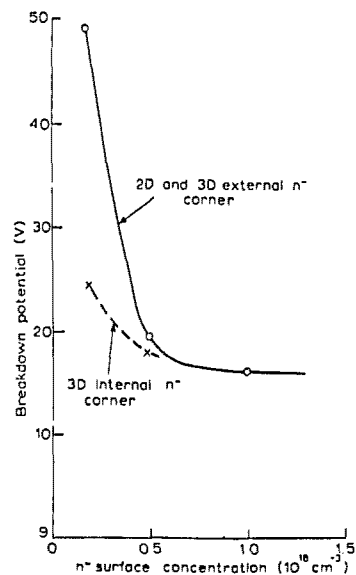


Fig 9. Breakdown potential for central section (2D) and external and internal corner (3D) v. n^- surface concentration